Arch. Metall. Mater. **69** (2024), 1, 9-16

DOI: https://doi.org/10.24425/amm.2024.147776

K. ABIB[1*], B. ALILI[1], T. BAUDIN[2], A.-L. HELBERT[2], F. BRISSET[2], L. LITYNSKA-DOBRZYNSKA[3], P. ZIEBA[3], D. BRADAI[1]

ON SOME FEATURES OF THE GRAIN AND SUBGRAIN SIZE IN A Cu-Cr-Zr ALLOY AFTER ECAP PROCESSING AND AGING

A Cu-1Cr-0.1Zr alloy has been subjected to ECAP processing via route Bc and aging at 250-800°C. Electron BackScatter diffraction (EBSD), Transmission Electron Microscopy (TEM) and X-Ray Diffraction Line Profile Analysis (XRDLPA) techniques have been used to unveil some peculiarities of the grain and subgrain structure with a special emphasis on the comparison of the grain size estimated by the three techniques. For the alloy ECAP processed and aged up to 16 passes, the grain size (from EBSD, $0.2 < d < 5$ µm), subgrain size (from TEM, $d \sim 0.75$ µm) and "apparent" average crystallite size (from XRDLPA, $d < 0.25$ µm) are manifestly different. The results were compared to the published data and analyzed based on the fundamental aspects of these techniques.

Keywords: Cu-Cr-Zr; ECAP; EBSD; XRDLPA; TEM

1. Introduction

Cu-Cr-Zr alloys are mainly used in electric/microelectronics and nuclear fusion reactors [1]. The high conductivity of the alloy is ascribed to the low solubility of Cr and Zr in copper at room temperature [2], and its strength is due to the precipitation of Cr clusters and Cu_xZr_y phases in the copper matrix [3,4].

The structure, precipitation sequence, thermal stability and mechanical properties of Cu-based alloys after severe plastic deformation (SPD) have been extensively studied [5-12]. SPD is a way to generate significant grain refinement [13]. The main result of SPD processing is a considerable and complex grain fragmentation and subdivision owing to the considerable hydrostatic pressure and changes of the deformation path [13].

EBSD technique has been confirmed a powerful tool to highlight the peculiarities of grain and subgrain size evolution even at moderate to high strain [14-18]. In practice, the highly-strained microstructure of SPD materials may be characterized only locally by TEM. TEM methods are very suitable to study the evolution of nanograins by quantitative analysis of their structural morphology including grain subdivision, boundary spacing and boundary misorientation [13].

Moreover, XRDLPA has an overall advantage in providing detailed information on the mean crystallite size, the crystallite size distribution, the internal microstrains and the related dislocation densities [8,9]. Thus, a comprehensive characterization of the microstructure may be achieved most easily through a simultaneous application of EBSD, TEM and XRDLPA.

However, in the literature, an evaluation and/or discussion about the characteristic difference between the grain and subgrain size after SPD processing and aging, provided by the three techniques, is still lacking.

The present study attempts to fill this lack in Cu-1Cr-0.1Zr (wt.%) alloy after SPD processing by ECAP and aging at temperature ranging from 250 to 800°C for 1 and 4 h using EBSD, TEM and XRDLPA techniques.

2. Experimental procedure

The material considered in this study is a commercial Cu-1Cr-0.1Zr (wt.%) alloy that was supplied in the form of rod bars by Goodfellow (UK). Billets of 10 mm diameter and 60 mm length were then machined for ECAP processing and solution heat-treated for 1 h at 1040°C in a protective inert gas

[1] UNIVERSITY OF SCIENCES AND TECHNOLOGY HOUARI BOUMEDIENE, FACULTY OF PHYSICS, BP 32 EL ALIA, BAB EZZOUAR, ALGIERS, ALGERIA
[2] UNIVERSITY PARIS-SACLAY, ICMMO, 91405, ORSAY, FRANCE
[3] INSTITUTE OF METALLURGY AND MATERIALS SCIENCE, POLISH ACADEMY OF SCIENCES, 25 REYMONTA STR., 30-059 KRAKOW, POLAND

* Corresponding author: abib_khadidja@yahoo.com

atmosphere followed by a subsequent water quenching. The rods were then processed by ECAP at room temperature up to 1 and 16 passes using route B_c. The full details of the ECAP processing can be found in references [11, 12]. After ECAP processing, annealing was carried out at 250-800°C for 1 and 4 h under high vacuum.

After ECAP processing, the samples for EBSD (slices of 1 mm thickness) were cut near the center of the ECAP billets in a plane parallel to the extrusion direction (Sample 1 in Fig. 1). After ECAP processing and aging, discs of 1 mm thickness (Sample 2 in Fig. 1) were cut perpendicularly to the axis of the cylindrical billet and then mechanically polished with 0.02 μm colloidal silica solution. EBSD measurements were performed for ECAPed and ECAPed and annealed samples on the transverse plane (ND-ED) by means of a Scanning Electron Microscope (SEM) with a Field Emission Gun JEOL JSM-7001F (at a 20 kV voltage) using HKL Channel 5 Oxford Instruments software and a Field Emission Gun (FEG) SUPRA 55 VP operated at 20 kV using the OIM^{TM} software, respectively. The collected EBSD data enabled the determination of the mean grain size, the grain size distribution and the distribution of the boundary misorientation angles [19].

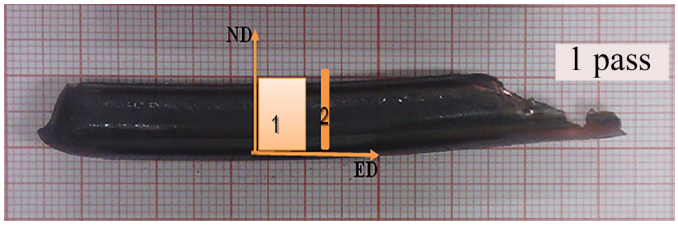

Fig. 1. Schematic illustration of the cutting of the ECAP samples: (1) and (2) refer to as ECAP processed and ECAP processed and aged conditions, respectively

Analytical transmission electron microscope FEI Tecnai G^2 at 200 kV equipped with high-angle annular dark-field scanning transmission electron microscopy detector HAADF-STEM and an energy dispersive X-ray EDAX spectrometer (EDS) was employed for microstructural (ultrafine grain size, precipitate size distribution, nature and volume fraction) characterization of the Cu-1Cr-0.1Zr (wt.%) alloy after various heat treatments. The TEM specimens were electro-polished using a Tenupol 5 twin jet polishing unit with an electrolyte of 75% HNO_3 and 25% CH_3OH. In HAADF-STEM experiments a spot size with a beam diameter of about 1 nm has been used. Thin foils were sectioned from the plane perpendicular to the working axis (ED) of the one-pass ECAPed sample and aged at 550°C for 4 hours.

The X-ray diffraction was conducted on flat and polished surfaces of each sample using an X'Pert-PRO PW 3040 Philips X-ray diffractometer (XRD) with CuKα radiation operating at 40 kV and 20 mA. In this analysis, the 2θ Bragg angle varied from 10 to 110°, the step scan was 0.02° and the counting time was 4s for each step. To investigate the dislocation density and the average crystallite size, the XRD patterns taken from ECAP processed samples were analyzed using the whole powder pattern modeling (WPPM) method implemented in PM2K code [20,21]. This non-destructive method provides information on specimen microstructure by directly comparing model-related XRD with experimental patterns. The main features of interest are the size and the shape of diffraction domains as well as the nature and concentration of lattice defects [22].

3. Results

The microstructure of the as-received and solution annealed Cu-1Cr-0.1Zr (wt.%) was described in [12]. The microstructure of the as-received alloy looked like a fibrous or columnar cast grain structure. The columnar structure exhibited lateral dimensions by far greater than transverse ones and following Rostoker et al. [23], such columnar-type structure resulted from strong thermal gradients expected in "chill" casting. After solution annealing at 1040°C during 1 h in an argon atmosphere, a granular microstructure (not shown here) with grains nearly equiaxed was formed ($d \sim 200$ μm) [12]. The grains were surrounded by quite irregular boundaries and contained a high fraction of annealing twins which very probably formed during the solution annealing at 1040°C for 1 hour [12].

Fig. 2 shows the EBSD maps Unique Grain Color mode of Cu-1Cr-0.1Zr (wt.%) alloy after ECAP processing to 1 passe and aging at 250, 400, 550 and 800°C for 1 hour. As already mentioned, the ECAP processing via route B_c produced a lamellar and elongated microstructure with grains extending their longitudinal dimension approximatively at 45° relatively to the extrusion direction (Fig. 2a) [12]. It is to be noted that the orientation maps and related herafter results associated with annealing at 400°C are not presented.

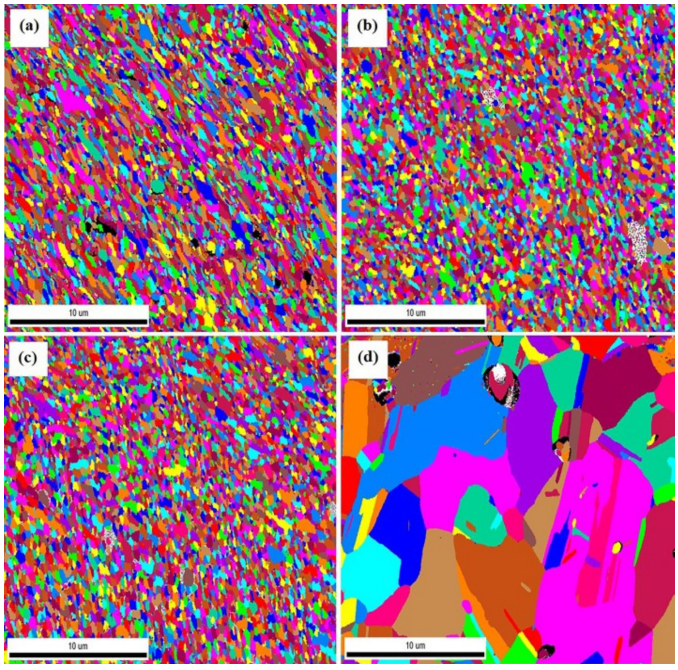

Fig. 2. EBSD maps in Unique Grain Color mode of Cu-1Cr-0.1Zr (wt.%) alloy after ECAP processing and aging for: a) 1 pass, b) 1 pass+250°C-1 h, c) 1 pass+550°C-1h and d) 1 pass+800°C-1 h, respectively

After one ECAP pass processing followed by annealing at 250, 550 and 800°C for 1 hour, the microstructure was almost similar upon increasing aging temperature (Figs. 2b-d). This microstructure was complex and duplex and characterized by a large deformed implemented area with small recrystallized grains. Such microstructure was ascribed to a probable particle stimulated nucleation (PSN) mechanism during recrystallization [11].

A noticeable and strong grain refinement occurred after 16 ECAP passes (Fig. 3a) due to considerable grain fragmentation [12]. The microstructure of the sample after 16 ECAP passes and aging at 250 and 550°C for 1 hour (Figs. 3b-c) exhibited a fine-grained structure inherited from severe plastic deformation that remained stable relatively to as-ECAPed state as shown in Fig. 3a. Annealing up to 800°C resulted (Fig. 3d) in a rapid and grain growth following a discontinuous mode of recrystallization as stated by Abib et al. [11].

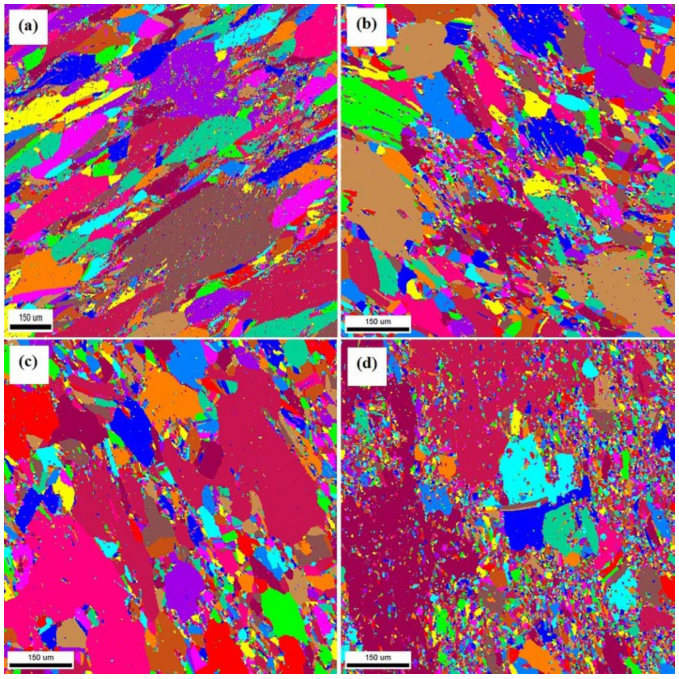

Fig. 3. EBSD maps in in Unique Grain Color mode of Cu-1Cr-0.1Zr (wt.%) alloy after ECAP processing and aging for: a) 16 passes, b) 16 passes+250°C-1 h, c) 16 passes+550°C-1 h and c) 16 passes+800°C-1 h, respectively

Figs. 4a and b show the histograms of grain size obtained by OIM-EBSD after 1-hour aging at 250, 400, 550 and 800°C for Cu-1Cr-0.1Zr alloy after 1 and 16 ECAP passes, respectively. Fig. 4a shows that for one ECAP pass and annealing at temperatures below 550°C. The ECAP structure remained remarkably fine-grained and stable during aging at temperatures up to 400°C whereas from 550°C there was a dual size distribution (almost bimodal distribution) corresponding to a population of unrecrystallized grains ($d \sim 200$ µm) and another corresponding to those already recrystallized and underwent grain growth ($d \sim 20$ µm). This is because ECAP processing up to 1 (and 16 passes) and annealing lead to a nano-precipitation of Cr clusters and Cu_5Zr phase that could strongly hinder the recrystallization process below 550°C [11]. It is worth noting that Abib et al. [12], have meticulously analyzed the grain size evolution and have adopted the definition of the microstructural parameters for the grain size evaluation from EBSD maps used by Tirsatine et al. [16]. The grain sizes were measured as the mean length (major axis, L) and thickness (minor axis, l) of the elongated grains estimated from the Line Intercept Method. Abib et al. [12] clearly stated that both decreased substantially to reach the value of $L = 0.73$ µm and $l = 0.43$ µm after 16 passes. No saturation was observed between 1 and 16 passes, while the value of grain aspect ratio (L/l) decreased from 2.14 after 1 ECAP pass to 1.69 after 16 passes, indicating that grains became more or less equiaxed as the ECAP pass number increased. Very fine and elongated microstructure in a similar alloy (Cu-0.44Cr-0.2Zr) after ECAP processing through route B_c up to 12 passes have been reported [5-7].

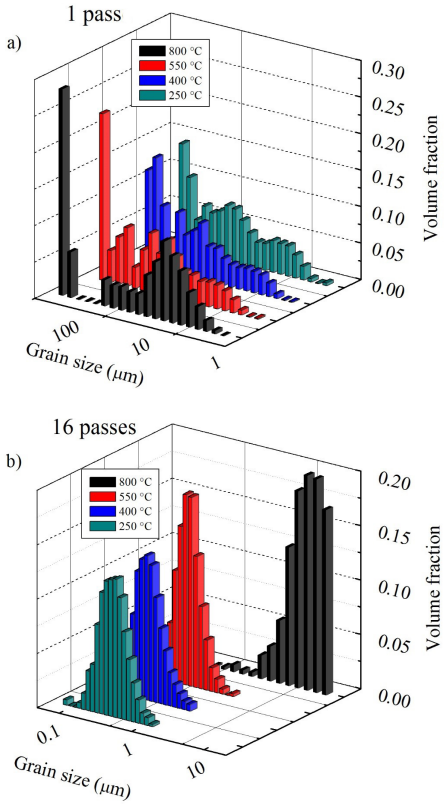

Fig. 4. Histograms showing the distribution of grain size of ECAP deformed Cu-1Cr-0.1Zr (wt.%) alloy and aged at 250, 400, 550 and 800°C for 1 h. a) 1 pass and b) 16 passes

Fig. 4b shows the changes in grain size obtained by OIM-EBSD after 1-hour aging at 250, 400, 550 and 800°C temperatures for Cu-1Cr-0.1Zr alloy after 16 ECAP passes. At 250, 400 and 550°C, grain size appears to be stable ($d \sim 0.2$ µm) and then there is a clear change in the histogram corresponding to 800°C aging, where a net tightening around a mean grain size of 5 µm is clearly noticed. This feature is a mark of a recrystallization and grain growth process.

The discrepancy between the finding associated with the sub-grain size of Vinogradov et al. [5-7] with the present data

presented in Figs. 2a and 3a may be explained by the difference in the definition of the grain size measured by EBSD and TEM techniques. In the case of EBSD map, each grain, with a certain grain tolerance angle (2° in the present study), is randomly colored, while in a TEM pattern, grain or subgrain with deformation features are directly observed. It is worth noting that in EBSD, the grain size may also be specified by a diameter. The diameter of a particular grain is calculated by determining the area of a grain and then assuming the grain is a circle [24].

The conventional TEM bright-field image of the Cu-1Cr--0.1Zr (wt.%) alloy after ECAP processing to one pass and aging at 550°C for 4 hours shows a microstructure of typical ultrafine-grained microstructure with an average size of about 0.75 ± 0.15 μm (Fig. 5a). Vinogradov et al. [5] have reported quite lower values (~0.160 μm) in a Cu-0.44Cr-0.2Zr alloy after ECAP processing (route Bc) to 12 passes. Khereddine et al. [14] have also reported very low subgrain size (down to 0.450 μm) estimated from TEM in a Cu2.3Ni-0.5Si alloy after ECAP processing using Route A up to 12 passes.

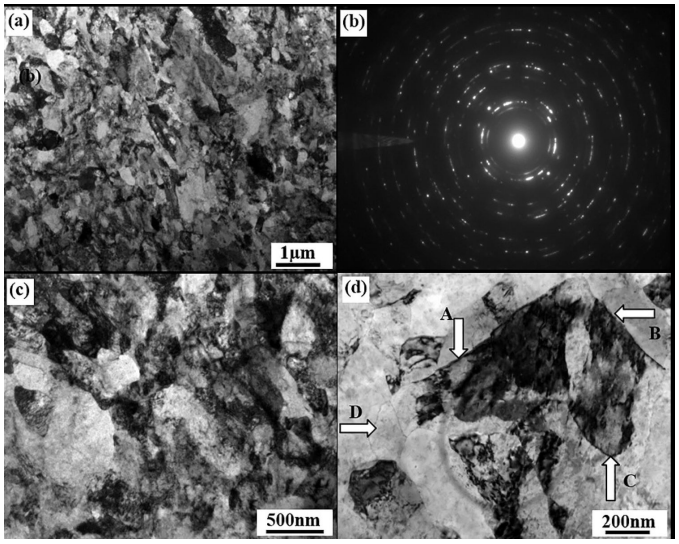

Fig. 5. (a) TEM bright-field image of the Cu-1Cr-0.1Zr (wt.%) alloy after ECAP processing to 1 pass and aging at 550°C for 4 h, b) SAED pattern corresponding to the analyzed area, c-d) higher magnifications showing peculiar details of non-equilibrium grain boundaries shown by arrows in d)

Enhanced magnification shows that the microstructure (Fig. 5c) consists of dislocation-free sub-grains with sharp (high-angle) boundaries and zones of moderate-to-high distortions and dislocation walls (low-angle boundaries). Grain boundaries are not easily detectable due to the existence of high dislocation density in their neighborhood. Many similar observations were reported in the literature after SPD processing and aging of Cu-based alloys [25,26]. Higher magnifications showing peculiar details of non-equilibrium grain boundaries are presented by arrows in Fig. 5d. Non-equilibrium grain boundaries are typical for different materials after SPD processing, and their role in the mechanical behavior of UFG materials has been discussed in many reports [27,28].

The SAED pattern (Fig. 5b) shows reflections along the rings, typical of a fine-grained polycrystalline material. The visible rings are not continuous, which means that the preferred orientation of the planes occurs during the ECAP process. In the SAED pattern, the azimuthal spreading of spots is also consistent with the presence of internal stresses after processing by ECAP. As already stated by Vingradov et al. [5] the disordered dislocation arrangement is energetically unfavorable, and dislocations are irregularly distributed so that the small grains are rather dislocation-free and most of them are trapped in the grain boundaries, leading to high internal stresses regions.

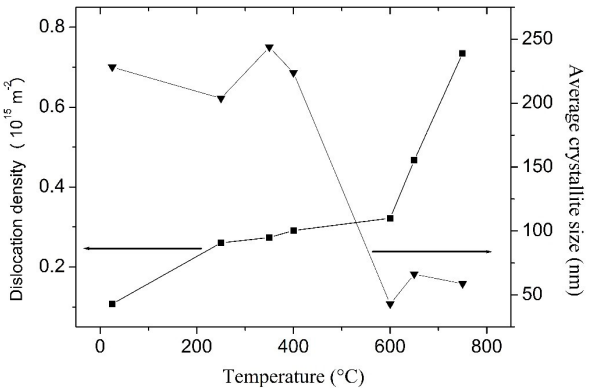

Fig. 6. Dislocation density and "apparent" average crystallite size in ECAP deformed to 4 passes Cu-1Cr-0.1Zr (wt.%) alloy and aged at 250-800°C for 1 h

The evolution of the "apparent" average crystallite size (in the literature of XRDLPA the average grain size in the direction of diffraction vector is also called "column length" following the definition of [22] and the concept of column length ideally considers grain in a polycrystalline system as made of a column of cells along the scattering direction) and the dislocation density in ECAP deformed to 4 passes Cu-1Cr-0.1Zr (wt.%) alloy and aged at 250-800°C for 1h are presented in Fig. 6. The results for the remaining specimens (1 and 16 passes) exhibited quite similar trends and therefore are not presented here.

Manifestly, both curves exhibit a breakdown near 550°C where the dislocation density decreased its initial value by 75% and the average domain size raised considerably (more than 200%). These trends are in total agreement with the findings of Abib et al. [11] who studied the thermal stability of the same alloy after ECAP processing and aging at the same temperatures. These authors evidenced a collapse of the hardness during isochronal annealing around 550-600°C. This collapse was ascribed to recrystallization and grain growth phenomena [29]. Gubicza et al. [30] have presented quite resembling plots for the dislocation density and average crystallite size in technical purity copper specimens after ECAP processing. Indeed, these authors studied the thermal stability of the ultrafine-grained microstructure by differential scanning calorimetry (DSC) and XRDLPA and evidenced a recovery process that occurred in the range of 240-310°C depending on the heating rate. Abib et al. [29] have stated that a complex precipitation sequence occurred during an-

nealing the ECAP deformed Cu-1Cr-0.1Zr (wt.%) alloy. This sequence could very plausibly delay the recovery-recrystallization process to higher temperatures (550-600°C for Cu-1Cr-0.1Zr (wt.%) alloy versus 240-310°C for technical pure Cu).

4. Discussion

The present investigation was conducted on a Cu-1Cr-0.1Zr (wt.%) alloy after ECAP processing and aging at 250-800°C for 1 and 4 hours using three different techniques for microstructural observations. The results show both agreements and also inconsistencies and it is essential to examine these apparent differences. It is worth noting that there was no intention to discuss the mechanisms which govern grain fragmentation or subgrain formation. Exhaustive details about the grain subdivision during ECAP processing can be found in the literature [30-34]. Only the achieved size and its evaluation through the three above-cited techniques will be considered here.

In this frame, one has to keep in mind some basic recommendations inspired by the literature. EBSD data collection and analysis are based on the definition of a “grain”. Indeed, a grain is generally defined as a continuous set of pixels in space (a dedicated algorithm groups sets of connected and similarly oriented points into “grains”), larger than a threshold value and bordered either by the edge of the map or by disorientation greater than a threshold. Threshold values should be carefully chosen by the user as grain size and distribution are closely dependent on them, especially when most interfaces are low misorientation grain boundaries [35]. An EBSD map is by essence a virtual transcription of real microstructural features under well-defined conditions. Especially, when high magnification is used to analyze the subgrain microstructure, it is strongly recommended to have large scan areas instead of small ones due to the existence of a maximum value of index points as a function of step size [36].

SPD processed materials have an extremely “fine-grained” structure. Following Hebesbberger et al. [37], this term has to be avoided since two adjacent grains should be separated by a ”true” grain boundary. This is not true for most SPD processed metals. Even at large misorientation angles, the subgrains seem to be separated by layers of finite thickness, which might be better described as arrangements of dislocations. Nazarov et al. [38] commonly used the term “non-equilibrium boundaries”. It is only after deformation at elevated temperatures or after subsequent annealing that grain boundaries in the classical sense are observed [39].

Indeed, Humphreys and Hatherley [40] stated that in an alloy of medium or high stacking fault energy (SFE), the dislocations are classically organized after deformation in the form of a three-dimensional cell structure. After subsequent annealing, owing to recovery, the tangled cell walls transform to more regular dislocation networks or low angle grain boundaries and the number of dislocations in the cell interiors also weakens. The cells become subgrains.

With the addition of Cr and Zr, the SFE of Cu-Cr-Zr alloy becomes lower than that of pure Cu [41]. The SFE of pure copper is 78 mJ/m^2 [42]. Under such conditions, the Cu-Cr-Zr alloy will probably behave quite differently after ECAP processing and aging and the microstructure will exhibit quite irregular and chaotic aspects as shown in Fig. 5.

As shown in Fig. 5d, some grain boundaries are mostly diffuse, indicating their non-equilibrium nature. The concept of non-equilibrium grain boundary was first defined by Valiev et al. [43,44] and then it has been used by many other researchers [45,46]. It refers to grain boundaries of materials with ultrafine-grained microstructures obtained through ECAP or high pressure torsion (HPT). Such grain boundaries have high densities of trapped lattice dislocations [47,48] and an elastically-distorted layer near the grain boundary.

Fig. 5 clearly shows a non-uniform microstructure in general and grain size scattering in particular. Indeed, as stated by An et al. [49], alloys with high SFE are characterized by a high rate of recovery and a rapid evolution into a uniform microstructure [9], whereas in the materials with low SFE, as in the case of Cu-Cr-Zr alloys, the recovery occurs slowly because of the significant difficulty of cross-slip.

One can speculate that the sub-grains size and “apparent” average crystallite size visible in Fig. 5 and 6 are quite different. The subgrain size assessed via TEM technique (~0.75 μm after ECAP processing to 4 passes and aging at 550°C for 4 hours) is, by far, greater than “apparent” crystallite size or coherently scattering domains obtained by XRDLPA (all estimated values are below 0.25 μm). This finding is in line with published data for bulk ultrafine-grained alloys produced by SPD techniques even if these data did not deal with aged specimens. Certainly, the grain size determined by TEM was about four to six times higher than the crystallite size obtained by XRDLPA [50-54]. TEM investigations indicated that the grains in SPD materials are divided into subgrains and/or dislocation cells which were separated from each other by low-angle grain boundaries. The crystallite size in SPD metals obtained by X-ray diffraction is equivalent to the mean “apparent” size of domains that scatter X-rays coherently. Consequently, X-ray diffraction makes a difference between the dislocation cells which are separated from each other by low misorientations, typically under 1-2°. It is well-known that one can “see” the dislocations cells whose walls desorieted by few degrees. However, the coherent diffraction domains are less defected than dislocation cell. XRDLPA anlysis concerns almost “pure” crystal in the sense dislocation-less. Whereras, in TEM, a sub-grao,n or a cell can conta dislocations which one may always not detect. Therefore, a coherent domain of diffraction is a subset of the cell, may be its sub-strucyure. Consequently, the TEM grain size is higher than the dislocation cell size obtained by XRDLPA [50,51]. Moreover, the size of the grains and/or subgrains measured on TEM micrographs is often smaller than those measured from EBSD maps. An other paradox may originate from technical consdiedations is the fact that EBSD technique is very prone to noise and is tributary of the image quality and confidence index parameters, Consequently,

a manifest underestimation of the grain size may occur during the data acquisition from grains having very small size since these may be biaised by "dark" indexed noises.

For Cu-Ni-Si alloy processed by ECAP and HPT techniques, TEM and XRDLPA (WPPM) techniques were used for microstructural evaluation and the results showed some coherency between these techniques [14]. Obviously, both HPT and ECAP samples led to a decrease in the mean domain size and an increase in the dislocation densities. As an example, the maximum domain size refinement revealed by XRDLPA obtained by HPT was around 40 nm after 3 turns ($\varepsilon \sim 40$) and 45 nm for ECAP samples processed after 12 passes ($\varepsilon \sim 6$). However, the latter authors have measured (using the TEM technique) quite larger value of the subgrain size that was close to 200 nm after ECAP processing up to 12 passes .

Contrarily, Scardi and Leoni [55] have established that the grain size distribution provided by TEM and XRDLPA (WPPM) techniques for a nanocrystalline Ni sample obtained by prolonged ball milling agreed remarkably. However, they stated also that grain size data may be different since XRD is sensitive to the size of coherently scattering crystalline domains, whereas TEM pictures do not always provide a clear distinction between grains and crystalline domains in highly defected metals.

Other XRDLPA method (Bayesian/Maximum Entropy) has been agreed in certifying a nanocrystallite-size standard reference material (SRM) that was developed at the National Institute for Standards and Technology (NIST) [55]. Indeed, developments in determining the nanocrystalline size distribution from X-ray line profile analysis have seen this method comparable to existing direct techniques such as TEM [55-57].

Globally, the overall values and trends of grain, sub-grain and cristallite sizes are almost in line with the published data. As a sounding example, Munõz et al. [58] have analyzed the microstructure of an ARMCO iron processed by 16 ECAP passes via EBSD, TEM and XRDLPA (MAUD for Material Analysis Using Diffraction). Quite different values of grain, sub-grain and crystallite sizes were obtained from each technique. The lower values were obtained by XRDLPA whereas two to three times higher values were achieved by TEM or EBSD techniques.

5. Conclusions

In this work, a Cu-1Cr-0.1Zr (wt.%) alloy was ECAP processed via route Bc up to 16 passes and aged at 250-800°C for 1 and 4 hours. Based on the experimental results, the following conclusions are drawn:

- Annealing up to 800°C for 1h resulted in a rapid grain growth ($d \sim 5$ μm) following a recrystallization after ECAP processing up to 16 passes.
- The conventional TEM bright-field image of the Cu-1Cr-0.1Zr (wt.%) alloy after ECAP processing to one pass and aging at 550°C for 4 hours shows a typical ultrafine-grained microstructure with an average size of about 0.75 ± 0.15 μm.
- The evolution of the "apparent" average crystallite size and the dislocation density in ECAP deformed to 4 passes Cu-1Cr-0.1Zr (wt.%) alloy and aged at 250-800°C for 1 h exhibited a breakdown near 550°C. The average crystal size raised considerably (more than 200%) and the dislocation density decreased its initial value by 75% between 250 and 800°C.
- For ECAP processed and aged Cu-Cr-Zr alloy up to 16 passes, the grain size (from EBSD, $0.2 < d < 5$ μm), subgrain size (from TEM, $d \sim 0.75$ μm) and "apparent" average crystallite size ($d < 0.25$ μm) are manifestly different..

Acknowledgements

The authors wish to heartily thank Prof. Jose Maria CABRERA from Polytecnia ETSEIB, Universidad Politécnica de Cataluña, for inviting and helping Miss K. ABIB during her several scientific stays.

REFERENCES

[1] D.J. Edwards, B.N. Singh, S. Tähtinen, Effect of heat treatments on precipitate microstructure and mechanical properties of a CuCrZr alloy. J. Nucl. Mater. **67-370**, 904-909 (2007). DOI: https://doi.org/10.1016/j.jnucmat.2007.03.064

[2] I.S. Batra, G.K. Dey, U.D. Kulkarni, S. Banerjee, Microstructure and properties of a Cu-Cr-Zr alloy. J. Nucl. Mater. **299**, 91-100 (2001). DOI: https://doi.org/10.1016/S0022-3115(01)00691-2

[3] I.S. Batra, G.K. Dey, U.D. Kulkarni, S. Banerjee, Precipitation in a Cu-Cr-Zr alloy. Mater. Sci. Eng. A **356**, 32-36 (2002). DOI: https://doi.org/10.1016/S0921-5093(02)00852-3

[4] H. Fuxiang, M. Jusheng, N. Honglong, G. Zhiting, L. Chao, G. Shumei, Y. Xuetao, W. Tao, L. Hong, L. Huafen, Analysis of phases in a Cu-Cr-Zr alloy. Scripta Mater. **48**, 97-102 (2003). DOI: https://doi.org/10.1016/S1359-6462(02)00353-6

[5] A. Vinogradov, V. Patlan, Y. Suzuki, K. Kitagawa, V.I. Kopylov, Structure and properties of ultra-fine grain Cu-Cr-Zr alloy produced by equal-channel angular pressing. Acta Mater. **50**, 1639-1651 (2002). DOI: https://doi.org/10.1016/S1359-6454(01)00437-2

[6] A. Vinogradov, Y. Suzuki, T. Ishida, K. Kitagawa, V.I. Kopylov, Effect of Chemical Composition on Structure and Properties of Ultrafine Grained Cu-Cr-Zr Alloys Produced by Equal-Channel Angular Pressing. Mater. Trans. **45**, 2187-2191 (2004). DOI: https://doi.org/10.2320/MATERTRANS.45.2187

[7] A. Vinogradov, K. Kitagawa, V.I.Kopylov, Fracture and Fatigue Resistance of Ultrafine Grain CuCrZr Alloy Produced ECAP. Mater. Sci. Forum **503-504**, 811-816 (2006). DOI: https://doi.org/10.4028/www.scientific.net/MSF.503-504.811

[8] Y.I. Bourezg, K. Abib, H. Azzeddine, D. Bradai. Investigation of recrystallization kinetics in hot-rolled Mg-La alloy using differential scanning calorimetry technique. Thermochim. Acta **686**, 178550 (2020). DOI: https://doi.org/10.1016/j.tca.2020.178550

[9] H. Azzeddine, B. Mehdi, L. Hennet, D. Thiaudiere, B. Alili, M. Kawasaki, T.G. Langdon, D. Bradai, An in situ synchrotron X-ray diffraction study of precipitation kinetics in a severely deformed Cu-Ni-Si alloy. Mater. Sci. Eng. A **597**, 288-294 (2014). DOI: https://doi.org/10.1016/j.msea.2013.12.092

[10] N. Liang, J. Liu, Y. Wang, J. Tao Wang, Y. Zhao, Y. Zhu, A multiscale architectured CuCrZr alloy with high strength, electrical conductivity and thermal stability. J. Alloys Compd. **735**, 25 1389-1394 (2018). DOI: https://doi.org/10.1016/j.jallcom.2017.11.309

[11] K. Abib, H. Azzeddine, K. Tirsatine, T. Baudin, A.L. Helbert, F. Brisset, B. Alili, D. Bradai, Thermal stability of Cu-Cr-Zr alloy processed by equal-channel angular pressing. Mater.Charact. **118**, 527-534 (2016). DOI: https://doi.org/10.1016/J.MATCHAR.2016.07.006

[12] K. Abib, J.A.M. Balanos, B. Alili, D. Bradai, On the microstructure and texture of Cu-Cr-Zr alloy after severe plastic deformation by ECAP. Mater.Charact. **112**, 252-258 (2016). DOI: https://doi.org/10.1016/J.MATCHAR.2015.12.026

[13] M.J. Zehetbauer, Y.T. Zhu, (Eds.) Bulk Nanostructured Materials, Wiley-VCH, Weiheim, Germany, 2009.

[14] A.Y. Khereddine, F. Hadj Larbi, M. Kawasaki, T. Baudin, D. Bradai, T.G. Langdon, An examination of microstructural evolution in a Cu–Ni–Si alloy processed by HPT and ECAP. Mater. Sci. Eng. A **576**, 149-155 (2013). DOI: https://doi.org/10.1016/j.msea.2013.04.004

[15] F. Hadj Larbi, H. Azzeddine, T. Baudin, F. Brisset, A-L. Helbert M. Kawasaki, D. Bradai, T.G. Langdon, Microstructure and texture evolution in a Cu–Ni–Si alloy processed by equal-channel angular pressing. J. Alloys Compd. **638**, 25, 88-94 (2015). DOI: https://doi.org/10.1016/j.jallcom.2015.03.062

[16] K. Tirsatine, H. Azzeddine, T. Baudin, A.-L. Helber, B. Alili, D. Bradai, Texture and microstructure evolution of Fe–Ni alloy after accumulative roll bonding. J. Alloys Compd. **610**, 352-360 (2014). DOI: https://doi.org/10.1016/j.jallcom.2014.04.173

[17] S. Boudekhani, H. Azzeddine, K. Tirsatine, T. Baudin, A.-L. Helbert, F. Brisset, B. Alili, D. Bradai, Microstructure, Texture, and Mechanical Properties of Ni-W Alloy After Accumulative Roll Bonding. J. of Mater. Eng. and Perf. (2018). DOI: https://doi.org/10.1016/J.JALLCOM.2014.04.173

[18] S. Koriche, S. Boudekhani-Abbas, H. Azzeddine, K. Abib, A.-L. Helbert, F. Brisset, T. Baudin, D. Bradai, On the groove pressing of Ni-W alloy: microstructure, texture and mechanical properties evolution. Kovove Mater. **56**, 313-323 (2018). DOI: https://doi.org/10.4149/km_2018_5_313

[19] F. Bachmann, R. Hielsher, H. Schaeben, Texture Analysis with MTex, Free and OpenSource Software ToolBox; Solid State Pheno. **160**, 6-68 (2010). DOI: https://doi.org/10.4028/www.scientific.net/SSP.160.63

[20] P. Scardi, M. Léoni, Whole Powder Pattern Modelling. Acta Cryst. Section **A58**, 190-200 (2002). DOI: https://doi.org/10.1107/S0108767301021298

[21] P. Scardi, M. Léoni, Diffraction Analysis of the Microstructure of Materials in E.J. Mittemeijer & P. Scardi (Ed.), Berlin Springer (2004).

[22] D. Balzar, N.C. Popa, Diffraction Analysis of the Microstructure of Materials. in E.J. Mittemeijer & P. Scardi (Ed.), Berlin Springer (2004).

[23] W. Rostoker, J.R. Dvorak, Interpretation of Metallographic Structures, Academic Press Inc. (London) Ltd. (1965).

[24] www.edax.com, OIM Analysis^{TM}/help.

[25] K.X. Wei, W. Wei, F. Wang, Q.B. Du, I. Alexandrov, J. Hu, Microstructure, mechanical properties and electrical conductivity of industrial Cu–0.5% Cr alloy processed by severe plastic deformation. Mater. Sci. Eng. A **528**, 1478-1484 (2014). DOI: https://doi.org/10.1016/j.msea.2010.10.059.

[26] J. Wongsa-Ngam, M. Kawasaki,Y. Zhao, T.G. Langdon, Microstructure evolution and mechanical properties of a Cu–Zr alloy processed by high-pressure torsion. Mater. Sci. Eng. A**528**, 7715-7722 (2011). DOI: https://doi.org/10.1016/j.msea.2011.06.056

[27] R.Z. Valiev, A.A. Nazarov, In: M.J. Zehetbauer, Y.T. Zhu, (Eds.) Bulk Nanostructured Materials, Wiley-VCH Verlag GmbH & Co. KGaA, Weinheim (2009).

[28] R.Z. Valiev, E.V. Kozlov, Ivanov, F. Yu, J. Lian, A.A. Nazarov, B. Baudelet, Deformation behaviour of ultra-fine-grained copper. Acta Metall. Mater. **42**, 2467 (1994). DOI: https://doi.org/10.1016/0956-7151(94)90326-3

[29] B. Alili, H. Azzeddine, K. Abib, D. Bradai, Texture evolution in AZ91 alloy after hot rolling and annealing. Trans. Nonferrous Met. Soc. China. **23**, 2215-222 1(2013). DOI: https://doi.org/10.1016/S1003-6326(13)62720-X

[30] J. Gubicza, L. Balogh, R.J. Hellmig, Y. Estrin, T. Ungar, Dislocation structure and crystallite size in severely deformed copper by X-ray peak profile analysis. Mater. Sci. Eng. A **400-401**, 334-338 (2005). DOI: https://doi.org/10.1016/j.msea.2005.03.042

[31] R.Z. Valiev, R.K. Islamgaliev, I.V. Alexandrov, Bulk nanostructured materials from severe plastic deformation. Progr. Mater. Sci. **45**, 103-189 (2000). DOI: https://doi.org/10.1016/S0079-6425(99)00007-9

[32] V.M. Segal, V.I. Reznikov, V.I. Kopylov, D.A. Pavlik, V.F. Malyshev, Processes of plastic structure formation of metals. Science and Engineering Publishers House, Minsk, 1994.

[33] Y. Iwahashi, Z. Horita, M. Nemoto, T.G. Langdon, An investigation of microstructural evolution during equal-channel angular pressing. Acta Mater. **45**, 4733 (1997). DOI: https://doi.org/10.1016/S1359-6454(97)00100-6

[34] S.D. Terhune, Z. Horita, M. Nemoto, Y. Li, T.G. Langdon, T.R. McNelley. In T. Sakai, H.G. Suzuki (Ed.), Proceedings of the 4th International Conference on Recrystallization and Related Phenomena. The Japan Institute of Metals, 1999.

[35] F. Brisset, EBSD, Analyse et diffraction des électrons rétrodiffusés, Application et techniques couplées, EDP Sciences, France (2015).

[36] Y.J. Chen, J. Hjelen, H.J. Roven, Application of EBSD technique to ultrafine grained and nanostructured materials processed by severe plastic deformation: Sample preparation, parameters optimization and analysis.Trans. Nonferrous Met. Soc. China **22**, 1801-1809 (2012). DOI: https://doi.org/10.1016/S1003-6326(11)61390-3

[37] T. Hebesberger, H.P. Stûwe, A. Vorhauer, F. Wetscher, R. Pippan, Structure of Cu deformed by high pressure torsion. Acta Mater. **53**, 393-402 (2005). DOI: https://doi.org/10.1016/j.actamat.2004.09.043

[38] A.A. Nazarov, A.E. Romanov, R.Z. Valiev, On the structure, stress fields and energy of nonequilibrium grain boundaries. Acta Metall. Mater. **41**, 1033-1040 (1993).
DOI: https://doi.org/10.1016/0956-7151(93)90152-I

[39] N.A. Akhmadeev, N.P. Kobelev, R.R. Mulgukov, Y.M Seifer, R.Z. Valiev, The effect of heat treatment on the elastic and dissipative properties of copper with the submicrocrystalline structure. Acta Metall. Mater. **41**, 1041-1046 (1993).
DOI: https://doi.org/10.1016/0956-7151(93)90153-J

[40] F.J. Humphreys, M. Hatherley, Recrystallization and Related Phenomena, Oxford, Pergamon, 1995.

[40] K. Kapoor, D. Lahiri, I.S. Batra, S.V.R. Rao, T. Sanyal, X-ray diffraction line profile analysis for defect study in Cu-1 wt.% Cr-0.1 wt.% Zr alloy. Mater. Char. **54**, (2) 131-140 (2005).
DOI: https://doi.org/10.1016/j.matchar.2004.09.009

[41] R. Kočiško, T. Kvačkaj, A. Kováčová, D. Šimčák, R. Bidulský, M. Lupták, M. Vlado, I. Pokorný, The mechanical properties of OFHC copper and CuCrZr alloys after asymmetric rolling at ambient and cryogenic temperatures, Open Eng. **8**, 426-431 (2018).
DOI: https://doi.org/10.1515/eng-2018-0041

[42] R.Z. Valiev, A.V. Korznikov, R.R. Mulyukov, Structure and properties of ultrafine-grained materials produced by severe plastic deformation. Mater. Sci. Eng. **A168**, 141-148 (1993).
DOI: https://doi.org/10.1016/0921-5093(93)90717-S

[43] R.Z. Valiev, V.Y. Gertsman, O.A. Kaibyshev, The role of non-equilibrium grain boundary structure in strain induced grain boundary migration (recrystallization after small strains). Scr. Metall. **17**, 853-856 (1983).
DOI: https://doi.org/10.1016/0036-9748(83)90248-X

[44] Z. Horita, D.J. Smith, M. Nemoto, R.Z. Valiev, T.G. Langdon, Observations of grain boundary structure in submicrometer-grained Cu and Ni using high-resolution electron microscopy. J. Mater. Res. **13**, 446-450 (1998).
DOI: https://doi.org/10.1557/JMR.1998.0057

[45] Z. Horita, D.J. Smith, M. Furukawa, M. Nemoto, R.Z. Valiev, T.G. Langdon, An investigation of grain boundaries in submicrometer-grained Al-Mg solid solution alloys using high-resolution electron microscopy. J. Mater. Res. **11**, 1880-1890 (1996).
DOI: https://doi.org/10.1557/JMR.1996.0239

[46] J. Wang, Y. Iwahashi, Z. Horita, M. Furukawa, M. Nemoto, R.Z. Valiev, T.G. Langdon, An investigation of microstructural stability in an Al-Mg alloy with submicrometer grain size. Acta Mater. **44**, 2973-2982 (1996).
DOI: https://doi.org/10.1016/1359-6454(95)00395-9

[47] Z. Horita, T. Fujinami, M. Nemoto, T.G. Langdon, Equal-channel angular pressing of commercial aluminum alloys: Grain refinement, thermal stability and tensile properties. Metall. Mater. Trans. A **31**, 691-701 (2000).
DOI: https://doi.org/10.1007/s11661-000-0011-8

[48] X.H. An, S.D. Wu, Z.F. Zhang, R.B. Figueiredo, N. Gao, T.G. Langdon, Evolution of microstructural homogeneity in copper processed by high-pressure torsion. Scripta Materialia **63**, 560-563 (2010).
DOI: https://doi.org/10.1016/j.scriptamat.2010.05.030

[49] A.P. Zhilyaev, J. Gubicza, G. Nurislamova, Á. Révész, S. Suriñach, M.D. Baró, T. Ungár, Microstructural characterization of ultrafine-grained nickel. Phys. Stat. Sol. (a) **198**, 263-271 (2003).
DOI: https://doi.org/10.1002/pssa.200306608

[50] G. Ribarik, J. Gubicza, T. Ungar, Correlation between strength and microstructure of ball-milled Al–Mg alloys determined by X-ray diffraction. Mater. Sci. Eng. A **387-389**, 343-347 (2004).
DOI: https://doi.org/10.1016/j.msea.2004.01.089.

[51] Y.T. Zhu, J.Y. Huang, J. Gubicza, T. Ungar, Y.M. Wang, E. Ma, R.Z. Valiev, Nanostructures in Ti processed by severe plastic deformation. J. Mater. Res. **18**, 1908-1917 (2003).
DOI: https://doi.org/10.1557/JMR.2003.0267

[52] T. Ungar, J. Gubicza, G. Ribarik, A. Borbely, Crystallite size distribution and dislocation structure determined by diffraction profile analysis: principles and practical application to cubic and hexagonal crystals. J. Appl. Crystallogr. **34**, 298-310 (2001).
DOI: https://doi.org/10.1107/S0021889801003715

[53] J. Gubicza I.C. Dragomir, G. Ribarik, Y.T. Zhu, R.Z. Valiev, T. Ungar, Microstructure of severely deformed titanium from X-ray diffraction profile analysis. Mater. Sci. Forum **414-415**, 229-234 (2003).
DOI: https://doi.org/10.4028/www.scientific.net/MSF.414-415.229

[54] C.E. Krill, R. Birringer, Estimating grain-size distributions in nanocrystalline materials from X-ray diffraction profile analysis. Phil. Mag. A **77** (8), 621-640 (1998).
DOI: https://doi.org/10.1080/01418619808224072

[55] J.I. Langford, D. Louër, P. Scardi, Effect of a crystallite size distribution on X-ray diffraction line profiles and whole-powder-pattern fitting. J. Appl. Cryst. **33**, 964-674 (2000).
DOI: https://doi.org/10.1107/S002188980000460X

[56] N. Armstrong, W. Kalceff, J.P. Cline, J. Bonevich, J. Res. Nat. Inst. Stand. Techn. 2001; Proceedinds of Accuracy in Powder Diffraction III;, NIST; Gaitherburg, USA (2001).

[57] J.A. Muñoz, O.F. Higuera, J.A. Benito, D. Bradai, T. Khelfa, R.E. Bolmaro, A. Moreira, J. Jr. Mat. Sci. Eng. A **740-741**, 108-120 (2019). DOI: https://doi.org/10.1016/j.msea.2018.10.100